frontiers in Earth Science

ORIGINAL RESEARCH
published: 07 June 2019
doi: 10.3389/feart.2019.00114

Variability in the Gas Composition of the Popocatépetl Volcanic Plume

Noémie Taquet[1], Wolfgang Stremme[1], Michel Grutter[1], Jorge Baylón[1], Alejandro Bezanilla[1], Benedetto Schiavo[1], Claudia Rivera[1,2], Robin Campion[3], Thomas Boulesteix[4], Amiel Nieto-Torres[5], Ramón Espinasa-Pereña[5], Thomas Blumenstock[6] and Frank Hase[6]*

[1] Centro de Ciencias de la Atmósfera, Universidad Nacional Autónoma de México, Mexico City, Mexico, [2] Facultad de Química, Universidad Nacional Autónoma de México, Mexico City, Mexico, [3] Departamento de Vulcanologia, Instituto de Geofisica, Universidad Nacional Autónoma de México, Mexico City, Mexico, [4] Laboratorio Nacional de Geoquímica y Mineralogía, Universidad Nacional Autónoma de México, Mexico City, Mexico, [5] Centro Nacional de Prevención de Desastres, Mexico City, Mexico, [6] Institute of Meteorology and Climate Research, Karlsruhe Insitute of Technology, Karlsruhe, Germany

OPEN ACCESS

Edited by:
Nicole Bobrowski, Universität Heidelberg, Germany

Reviewed by:
Giancarlo Tamburello, National Institute of Geophysics and Volcanology (INGV), Italy
Michael Robert Carroll, University of Camerino, Italy

***Correspondence:**
Noémie Taquet
noemi.taquet@gmail.com

Specialty section:
This article was submitted to Volcanology, a section of the journal Frontiers in Earth Science

Received: *06 October 2018*
Accepted: *30 April 2019*
Published: *07 June 2019*

Citation:
Taquet N, Stremme W, Grutter M, Baylón J, Bezanilla A, Schiavo B, Rivera C, Campion R, Boulesteix T, Nieto-Torres A, Espinasa-Pereña R, Blumenstock T and Hase F (2019) Variability in the Gas Composition of the Popocatépetl Volcanic Plume. Front. Earth Sci. 7:114. doi: 10.3389/feart.2019.00114

Long-term time series of volcanic plumes composition constitute valuable indicators of the evolution of the magmatic and volcanic systems. We present here a 4-years long time series of molecular ratios of HF/HCl, HCl/SO_2, SiF_4/SO_2, HF/SiF_4 measured in the Popocatépetl's volcanic plume using ground-based solar absorption FTIR spectroscopy. The instrument, based in the Altzomoni NDACC (Network for the Detection of Atmospheric Composition Change) station, facing the Popocatépetl volcano, provides an unrivaled precision. The computed mean and standard deviation of the HF/HCl and HCl/SO_2 ratios for this period were found to be 0.24 ± 0.03 and 0.11 ± 0.03, respectively. SiF_4 was detected in three occasions and the SiF_4/SO_2 ratios ranged between $(1.9 \pm 0.5) \times 10^{-3}$ and $(9.9 \pm 0.4) \times 10^{-3}$. The HBr/HCl and HBr/$SO_2$ ratios remained below their detection limits (1.25×10^{-4} and 1.25×10^{-5}, respectively), given that a part of the HBr has already been converted to other bromine species (e.g., BrO, Br_2) a few kilometers downwind of the crater. Combining our time series with satellite SO_2 fluxes and seismic data, we explain the significant long-term HCl/SO_2 variations by changes in the conduit and edifice permeabilities, impacting the deep and shallow degassing processes. The high temporal resolution of the data also allows capturing the variation of the volcanic plume composition preceding and induced by a common moderate explosion at Popocatépetl volcano. We interpret the observed variations of the HCl/SO_2 ratio during the explosion in terms of changes in the contribution of the deep/shallow degassing. We additionally report the detection of an increase of SiF_4 after the explosion, likely explained by in-plume HF-ash interaction. During this event, SiF_4/HCl vs. HF/HCl was found to have a linear relation with a slope of −1/4, which implies a conservation of fluorine.

Keywords: SO_2, HCl, SiF_4, solar absorption, FTIR spectroscopy, volcanic gas, Popocatépetl

1. INTRODUCTION

Changes in the eruptive dynamics (passive degassing, dome extrusion, or destruction) of dome-capped volcanic systems are mainly controlled by the gas content in the magma, directly affecting its viscosity and ascending speed (Martel and Schmidt, 2003; Boudon et al., 2015; Manga et al., 2018). Magma mixing in the storage reservoir (Witter et al., 2005), assimilation of the volcanic edifice basement (Goff et al., 2001), gas redox reactions and gas-rock interactions (Love et al., 1998; Mori et al., 2002; Stremme et al., 2011; Battaglia et al., 2019), conduit permeability changes (Edmonds et al., 2001; Taquet et al., 2017; Campion et al., 2018), or hydrothermal activity and gas interactions in the volcanic gas plume (Bagnato et al., 2013) are important processes contributing to changes in the gas composition from the deep to the shallow system. The identification and estimation of the contribution of each of these individual processes require an ample database from long-term gas measurements. Ground-based FTIR spectroscopy allows long-term monitoring of the volcanic plumes composition (SO_2, HCl, HF, SiF_4) during both quiescent and eruptive periods and with sufficient temporal resolution to relate the composition change with both intrusive and eruptive processes.

The contrast in solubilities between the gas species (e.g., CO_2, SO_2, and halogens) and their variations during magma ascent are widely used to decipher the effusive-explosive transitions in eruptive processes (Aiuppa et al., 2009; Lee et al., 2018). Prior studies, some of which are also based on FTIR spectroscopic measurements, have already reported long-term but discontinuous time series of the halogen and sulfur contents in volcanic plumes. The long-term variability of the HCl/SO_2 ratio was previously related to both the deep and shallow disturbances of the volcanic activity, such as changes in the hydrothermal contribution (Hirabayashi et al., 1982; Mori and Notsu, 2008; Shinohara et al., 2015) or changes in the composition of the magmatic source (Oppenheimer et al., 2002). The short-term variations were rather explained by variations in the permeability of the magma column (Oppenheimer et al., 2002), lava domes growth or change in the lava extrusion rate (Edmonds et al., 2001). Trace gases such as SiF_4 in volcanic plumes were also studied (Francis et al., 1996; Love et al., 1998; Mori et al., 2002; Stremme et al., 2012; Taquet et al., 2017) for the understanding of the lava dome destruction episodes.

Considering the volcanic/magmatic factors likely to influence the plume composition, an open question is the extent to which variations in gas composition reflect the changes in the intrusive/extrusive contributions. Andesitic volcanoes with lava domes often behave cyclically, alternating magmatic episodes of extrusion and potentially hazardous episodes of dome destruction by volcanic explosions. Popocatépetl volcano has been one of the strongest permanent emitters of volcanic gases over its now 23-year long ongoing eruptive activity, and represents a potential risk for the 25 M inhabitants in its immediate neighborhood. As for most of the andesitic volcanoes, its regularly strong explosive activity impedes frequent direct observations and proximal gas composition measurements. The gas plume thus constitutes one of the only magmatic information purveyors.

In this contribution, we present a 4-years long time series of the HCl/SO_2, HF/HCl, and SiF_4/SO_2 ratios obtained from a high spectral resolution (HR) FTIR spectrometer, which forms part of the Network for the Detection of Atmospheric Composition Change (NDACC)[1], facing the Popocatépetl volcano. The variability of these time series is interpreted in the light of the SO_2 OMI-derived fluxes and of the volcanic activity described by both seismic records and visual observations.

2. BACKGROUND

The Popocatépetl volcano is an andesitic-dacitic stratovolcano (5,426 m a.s.l.) of the trans-Mexican volcanic belt, located 70 km SE of Mexico City (21 M inhabitants) and 43 km west of Puebla (3.2 M inhabitants). Although some historical plinian eruptions occurred in its past (the latest between 675 and 1095 A.D.; Siebe et al., 1996), its activity in the last century essentially consisted in the alternation of effusive and explosive phases with the extrusion of andesitic to dacitic lava domes until their destructions through series of vulcanian explosions (Gómez-Vazquez et al., 2016). The most recent historical eruptive phase before the current one started in 1919 and ended in 1927 (Gómez-Vazquez et al., 2016). The current eruptive phase started at the end of 1993, after 70 years of quiescence, with manifestations of phreatic activity related to the crater lake, which disappeared on December 1994 with the first important explosion. The first intra-crater lava dome was observed during March 1996, and since then at least 38 succeeded each other in the summit crater. Their growth is spasmodic, and occurs during very short extrusive episodes several hours to several days long, generally accompanied by low frequency harmonic tremor (Arambula et al., 2016) and explosive events. During an activity cycle, the lava dome endures multiple phases of successive inflation, degassing, deflation, and compaction, occasionally punctuated by its partial destruction. These processes lead to a progressive weakening of the dome structure, until the final destructive phase (days to weeks in duration), generally evidenced by series of consecutive moderate explosions. The Popocatépetl lava domes can reach highly variable volumes, estimated from 10^5 to 7×10^6 m^3 (Gómez-Vazquez et al., 2016), the most recent being smaller than those observed 20 years ago. Knowledge on the dome cycles of the current eruption only stems from seismic monitoring and the aerial photographs taken during rare overflights of the crater (Gómez-Vazquez et al., 2016), with the support of distant visible and infrared cameras. Only a few *in-situ* measurements were performed since the appearance of the first lava dome in 1996 (Goff et al., 1998, 2001), the composition measurements are thus principally based on remote sensing techniques.

The typical eruptive gas columns or passive degassing at Popocatépetl volcano are characterized by the presence of H_2O, CO_2, SO_2, HCl, HF, and SiF_4, the abundance of which was only sparsely measured since the volcanic reawakening in 1996 (**Table 3**). The most recent SO_2 fluxes estimations range from

[1]https://www2.acom.ucar.edu/irwg

3,000 to 5,000 ton/day for quiescent periods, and are higher than 25,000 ton/day for eruptive events (Delgado-Granados et al., 2001; Grutter et al., 2008; Campion et al., 2018) and show that the Popocatépetl's conduit system is essentially permeable (Campion et al., 2018). Ultimately, the variability of the SiF_4/SO_2 ratio was explored on the basis of high temporal resolution measurements (Taquet et al., 2017) to reveal the causes of transient permeability changes, highlighting the role of lava dome destruction episodes and short-term sudden drops in SO_2 fluxes preceding explosions (Campion et al., 2018).

These studies essentially provided snap shots of the composition of the Popocatépetl volcanic plume, but did not allow studying its variability over prolonged eruptive or passive degassing periods.

3. MEASUREMENTS AND METHODS

3.1. The Altzomoni Atmospheric Observatory

The measurements were performed between 2012 and 2016 from the Altzomoni Atmospheric Observatory (3,985 m a.s.l) (**Figure 1**), 12 km north of the Popocatépetl's crater. The site location has been chosen to comply with a number of spectroscopic and safety requirements, such as an open view to the volcano, a high altitude to minimize the water vapor and the anthropogenic contamination, a safe distance from the crater and the abundant ash-falls, the availability of power supply, communication and a convenient access (Stremme et al., 2011; Schiavo et al., 2019). In March 2012, a container equipped with a high resolution FTIR spectrometer coupled with a solar tracker was installed in the observatory. The instrument, the measurements and the retrieval products comply with the NDACC quality requirements, and provide high precision total columns and profiles of a wide range of atmospheric gases (Baylon et al., 2017). The site became an official NDACC station in 2015. Since October 2012, remote solar absorption measurements are performed every time the meteorologic and geometric conditions required for measurements are fulfilled. Solar occultation measurements of the Popocatépetl's plume can be performed on days with clear sky conditions and only during favorable wind conditions, which are typically fulfilled after the sunrise when the wind is toward the NE direction, so that the volcanic plume and the instrument are aligned with the sun (**Figure 1D**). More than one hundred measurement days out of the 591 recorded show a clear signal of the volcanic plume. Typically, the part of the volcanic plume measured by the instrument has traveled 10–20 km downwind from the crater and was recorded from a few minutes up to 1 h after being exhaled.

3.2. Instrumentation

The Bruker HR120/5 FTIR spectrometer (**Figure 1B**) is capable of measuring with a maximal optical path difference (OPDmax) and resolution (res) of 257 cm and 0.0035 cm^{-1}, respectively (res = 0.9/OPDmax). The spectrometer operates with either KBr or CaF_2 beam splitters, 3 different detectors (MCT, InSb, and InGaAs) and a set of 7 optical filters installed in a rotating wheel. The instrument is equipped with a precise solar tracker (Camtracker; Gisi et al., 2012) based on a commercial telescope mount as can be seen in **Figure 1A**. The system is equipped with an automated solar-tracker cover and liquid-nitrogen filling systems, which, together with a microwave communication system (50 km line of sight to the university campus), allows a fully-remote control of the instrument.

In general, the measurement sequence includes the acquisition of a pair of "low resolution" (0.1 cm^{-1}) spectra lasting several seconds and one with "high-resolution" (0.005 cm^{-1}), which can take as long as 7 min. In one sequence, this is repeated for each optical filter to cover the different spectral regions. The spectral resolution and filters used for each of the analyzed gases are reported in the **Table 1**. When the volcanic plume is detected, we can choose an alternative sequence that only consists of low resolution measurements, having NDACC filters 3 and 6 and near infrared (NIR) spectra measured with a higher frequency (**Table 1**). All the NIR spectra in both sequences are also measured with a "moderate resolution" (0.02 cm^{-1}), each of them taking 37 s.

3.3. Spectral Analysis

The analysis of SO_2, HCl, HF, SiF_4, HBr is optimized depending on the different optical filters used to measure the spectra and adapting the spectral resolution and the range for each of the different species (**Table 1**). HF and HCl are analyzed from NIR measurements (without filter) with moderate spectral resolution (0.02 cm^{-1}) and the InGaAS detector in DC (Direct Current) operation mode. HCl and SO_2 are retrieved together in the mid infrared (MIR) spectral range covered by the filter 3. SiF_4 and SO_2 are measured in the long wave IR spectral range using filter 6 with a spectral resolution of 0.1 cm^{-1}. The gas column amounts are retrieved from the measured spectra using the PROFFIT v.9.6 retrieval code (Hase et al., 2004). It solves the ray tracing and provides a forward simulation of the expected transmission spectra with line-by-line calculations using the cross sections and a priori profiles of each atmospheric constituent. The code makes the inversion by constrained least-squares fitting and the resulting vertical profiles and columns of the target gases are reported with a corresponding error analysis.

The retrieval strategies used for the analysis of the volcanic plume aimed specifically at optimizing the total column averaging kernel in the altitude of the volcanic layer between 5,500 and 6,000 m a.s.l. Therefore, a strategy for each specie is chosen depending if the gas has a stratospheric background or not, if more than one degree of freedom is allowed or if the available information is limited for its retrieval. SO_2 and SiF_4 do not have any atmospheric background and are retrieved as a simple scaling with contributions only on the lower levels. HF and HCl in the MIR region are retrieved adjusting the VMR-profile using a Tikhonov constraint on a logarithmic scale and an a priori which consists in the averaged profile of 41 years run of the Whole Atmospheric Community Climate Model (WACCM), as commonly done in the NDACC community, but with an increased concentration in the lower troposphere between 4 and 6 km. This strategy gives an initial sensitivity to the volcanic layer and allows adjusting both the stratospheric background and the volcanic plume. The HCl retrieval in the

FIGURE 1 | Presentation of the measurement site: The NDACC Altzomoni Atmospheric Observatory **(A)** Automated solar tracker installed on the roof of the station. **(B)** Picture of the high resolution FTIR spectrometer inside the container. **(C)** Location of the Altzomoni observatory, the seismic Canario station, and the Popocatépetl volcano. **(D)** A typical geometry for solar occultation measurements of the volcanic plume.

NIR region does not contain more than one independent portion of information and uses therefore a block-Tikhonov constraint shifting the VMR concentration below 6 km, while keeping the concentrations above 6 km fixed to the a priori calculated from the WACCM model.

For this study, a filter was applied to the data in order to only include the spectra that contain information of the volcanic plume. Measurements with SO_2 columns below 1.1×10^{16} molecules cm^{-2}, a baseline calculated over the 4 years of the record, were discarded. For the selected data, the HCl/SO_2 (Filter 3), HF/HCl (Open = no Filter) and SiF_4/SO_2 (Filter 6) ratios were determined for each day (or volcanic event) from the correlation plots of each pair of gases. The slopes were calculated when a good correlation is obtained (Pearson's coefficient $R \geqslant 0.8$). When the error in the slope (corresponding to 99% confidence intervals) is higher than 50%, the data are discarded. HF and SiF_4 columns were retrieved from spectra measured with different filters so that their ratios (SiF_4/HF) were derived from the SiF_4/HCl ratios (product of SiF_4/SO_2 and SO_2/HCl ratios) and HF/HCl ratios using interpolation in time. The retrieved slant columns within a volcanic plume are very sensitive to small movements of the plume with respect to the line of sight, but the interpolation of the gas ratios will not change as much as the individual columns. A calibration factor of 0.86 was applied to correct the HF/HCl ratio to account for spectroscopic inconsistency between the used line intensities of the fundamental and the first overtone of the HCl bands reported in the HITRAN 2004 spectral data base (Rothman et al., 2005).

3.4. OMI Fluxes

The SO_2 flux measurements used in this study were obtained by processing the standard NASA OMSO2 v2 product (Yang et al., 2007) with the traverse method (Bluth et al., 1994; Campion, 2014). The data from the OMSO2 product, downloaded from the Mirador server (https://mirador.gsfc.nasa.gov/), report SO_2 vertical column densities for each pixel of the image, obtained with four different SO_2 vertical distribution profiles (PBL: center of mass = 0.7 km; TRL: center of mass = 2.6 km; TRM: center of mass = 7.5 km; STL: center of mass = 15 km). The SO_2 content of the plume was interpolated for each pixel at the plume altitude between these four a priori values. Traverses are defined as rows or columns of pixels crossing the plume at increasing distances downwind from the crater. The SO_2 flux is calculated for each traverse as:

$$F = V.\cos(\theta).\sum_i C_i.L_i \quad (1)$$

Where V is the wind speed, θ is the angle between the traverse and the plume direction, C_i is the SO_2 column interpolated at the plume height for the ith pixel of the traverse, L_i is its length (or width depending on the plume direction). OMI's pixel size is 13×24 km at nadir, and stretches with increasing viewing angle, until reaching 16×140 km at the edge of the 2,500 km wide swath. The application of the traverse method requires two conditions in order to produce reliable results, which are a coherent plume transport direction and the absence of a cloud coverage above the volcanic plume. The fulfilling of the former condition can be assessed by a visual inspection of the SO_2 plume shape. The cloud top pressure and the cloud fraction, reported for each pixel as an ancillary information in the OMSO2 product, allow to assess the latest one. The values of SO_2 fluxes reported in **Figure 2C** are the average value of the fluxes measured on images fulfilling these two conditions. Despite taking the highest care in processing the OMI data, a systematic difference is observed between the OMI-derived SO_2 fluxes and those obtained using ground-based instruments such as COSPEC traverses. The ground-based measurements are in average 2.5 times higher than those of OMI but generally follow the same trends (Campion, in preparation). McCormick et al. (2014) compared such datasets for Tungurahua volcano, where roughly similar trends can be observed. The precise causes of this discrepancy are still under investigation although we suspect that the SO_2 column might be either underestimated by the

TABLE 1 | Filters, detectors, and spectroscopic parameters used for the analysis of SO_2, HCl, HF, SiF_4, and HBr in the Popocatépetl's plume from solar absorption measurements (LN2 = liquid nitrogen cooled).

Gas	Filter	Detector	Resolution (cm^{-1})	Spectral ranges (cm^{-1})
SO_2	3 & 4	InSb(LN2,DC)	0.1 & 0.005	2480.0–2520.0
SO_2	6	MCT(LN2,AC/DC)	0.1 & 0.005	1120.0–1180.0
HCl	3	InSb(LN2,DC)	0.1 & 0.005	2727.0–2728.5; 2775.0–2776.50; 2818.75–2820.35; 2820.75–2822.35; 2843.0–2844.4; 2903.35–2904.85; 2923.0–2924.50; 2925.0–2926.75; 2942.0–2943.5; 2960.3–2961.825; 2962.3–2964.0; 2995.0–2996.5
HCl	Open	InGaAs	0.02	5738.0–5740.0; 5767.0–5767.8; 5779.2–5779.9
HF	1, Open	InGaAs	0.1, 0.0075 & 0.02	3999.0–4003.5; 4036.5–4041.0
SiF_4	6	MCT(LN2,AC/DC)	0.1	1015.0–1035.0
HBr	3 & 4	InSb(LN2,DC)	0.005	2412.0–2413.75; 2432.0–2433.0; 2451.25–2453.00; 2488.0–2491.0; 2505–2510; 2541.0–2542.75; 2574.0–2576.0; 2589.95–2591.5; 2619.5–2623.0; 2634.0–2636.5; 2661.5–2664.0; 2673.9–2676.15; 2686.33–2688.05; 2697.4–2700.0; 2709.6–2710.7

OMI retrieval due to the high turbidity of the atmosphere over central Mexico or overestimated by the ground-based COSPEC measurements maybe due to a problem of calibration.

3.5. Seismic Data

Popocatépetl's seismic monitoring is operated by 3 triaxial broadband seismic stations of the CENAPRED (National Center for Disaster Prevention). The Canario station (2.1 km from the crater, 4,200 m.a.s.l.; **Figure 1C**), provides the data used in this study. We computed the Real-time Seismic Amplitude Measurement (RSAM) (Endo and Murray, 1991), consisting in the average amplitude of ground movements caused by volcanic events at 10 min intervals. As the RSAM does not differentiate between volcanic activity and other sources of ground vibration (wind, rain, thunder, or tectonic earthquakes), the data from Canario were filtered by manually removing non-volcanic signals from their waveform and frequency spectra. We manually reviewed more than 170,000 values for the study period comprising the period 2012–2016.

4. RESULTS

4.1. Variability of the Popocatépetl Plume Composition Over 4 Years

The complete time series of the HCl/SO_2, HF/HCl, and SiF_4/SO_2 ratios (error $\leqslant$50%) and their linear fit weighting-based errors are reported in **Figures 2A,B** concurrently with the SO_2 fluxes (**Figure 2C**) and seismic activity (**Figure 2D**).

4.1.1. HF/HCl

The measured HF and HCl columns are both detected and mutually sufficiently well correlated (Pearson's R $\geqslant$0.80, error $\leqslant$50%) in 77 out of 591 days of measurements and the corresponding slopes (HF/HCl) were reported with their error bars in **Figure 2A**. Gray and black colors distinguish data with an error lower than 10% (black, 34 measurement days) from the others with higher errors (gray, 43 measurement days). The following calculations are realized only selecting datapoints with an error lower than 10%. The HF/HCl ratios are distributed around an average value of 0.24 and a standard deviation of 0.03 (**Figure 3A**). Only 7% of the values are outside the standard deviation from the average. These values are essentially concentrated over short time periods (a maximum of 2 days) and do not systematically coincide with the RSAM "spikes" characterizing volcanic explosions in the seismic record or with shifts in the RSAM cumulative curve.

4.1.2. HCl/SO_2

The measured HCl and SO_2 columns are both detected and mutually sufficiently well correlated (Pearson's R $\geqslant$0.80, error $\leqslant$ 50%) in 129 out of 591 days of measurements, and their slopes (HCl/SO_2) are reported in **Figure 2B** with their error bars. As previously described for HCl/HF, data with error lower than 10% are represented in black (90 measurement days) and the other data in gray (39 measurement days) and the following statistical calculations are realized only using data with error lower than 10%. The mean and standard deviation obtained for the complete time series are 0.11 ± 0.03. The repartition of the HCl/SO_2 ratios relatively to the average (**Figure 3B**) shows at least three distinguishable periods, labeled period I (Nov. 2012–May 2013), II (Nov. 2013–Mar. 2014), and III (Sep. 2014–Dec. 2016), with different HCl/SO_2 averages reported in **Table 2**.

About 90% of the HCl/SO_2 ratios obtained during period I (Nov. 2012–May 2013) are below the overall average (0.11) with a mean ratio and standard deviation of 0.07 ± 0.02. A zoom of this period is presented in **Figure 4**. This period, displaying the most intense volcanic activity of the whole survey, is characterized by a monotonously declining trend of the ratio between values of 0.09 and 0.04, independent of the volcanic activity. The HCl/SO_2 declining trend (slope $= -0.34$%/day and $R^2 = 0.70$) was calculated after excluding iteratively outliers using the Chauvenet's criterion. Therefore, in each iteration a straight line is fitted and only the data with differences within the two

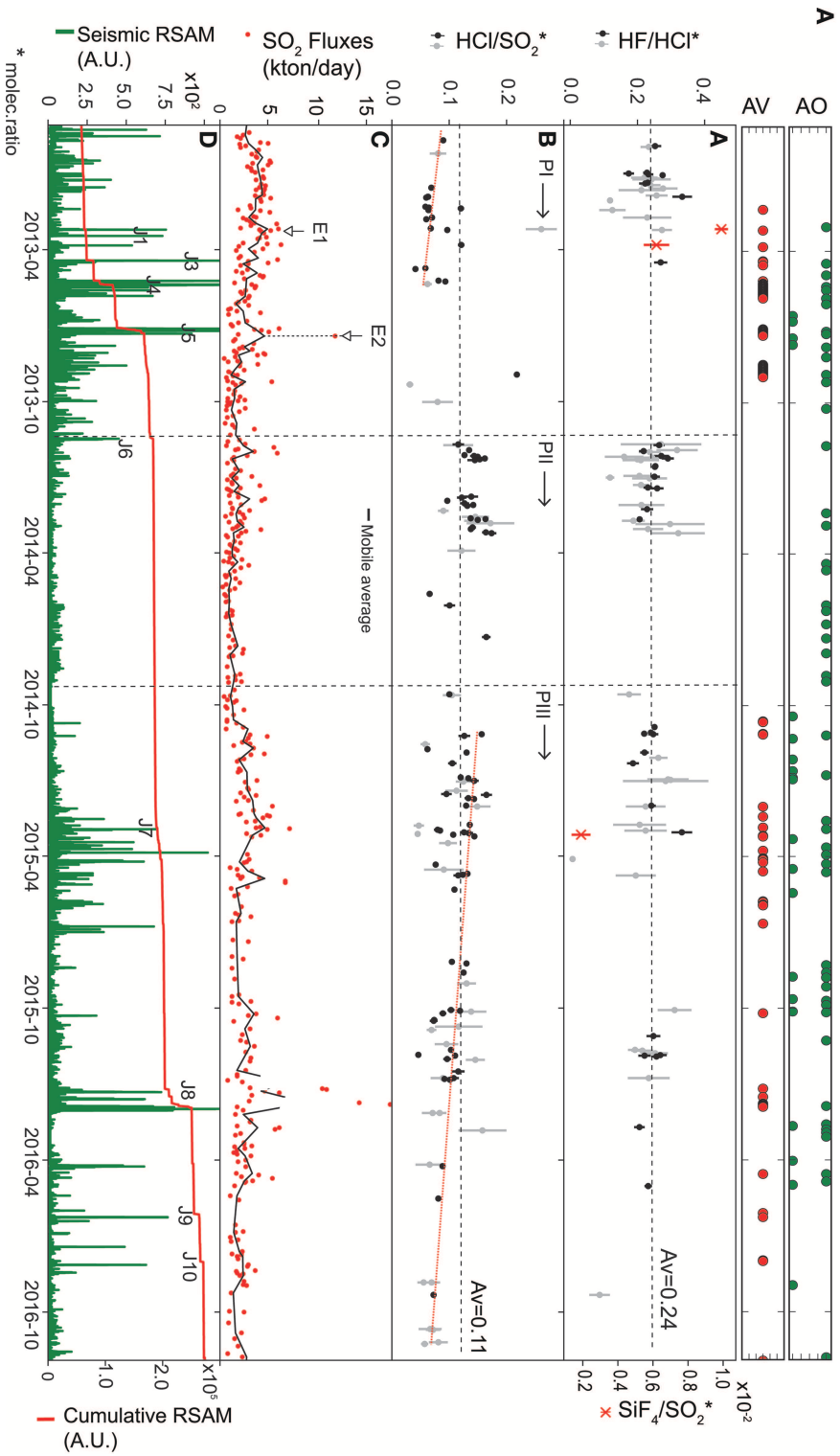

FIGURE 2 | Time series of the Popocatépetl plume composition between 2012 and 2017 for **(A)** SiF_4/SO_2 (red) and HF/HCl molecular ratios (black for datapoints with error $\leqslant$10% and gray for those with error $\geqslant$10%) **(B)** HCl/SO_2 molecular ratios (black for datapoints with error $\leqslant$10% and gray for those with error $\geqslant$10%), obtained from FTIR solar absorption measurements. The vertical dashed lines represent the beginning of each of the period PI, PII and PIII defined in **Table 2**. **(C)** SO_2 fluxes obtained from the OMI satellite measurements (red) and their moving average (black) over 5 points **(D)** seismic RSAM (green) and its cumulative curve (red) obtained from the Canario seismic station. J1–J10 indicate the main cumulative RSAM shifts. Top of the figure: AO, Aerial observations including overflights of the Popocatépetl crater and satellite observations from USGS. The presence of a lava dome is indicated by the position of the point (Top = Yes, Bottom = No). AV, Ash Venting episodes.

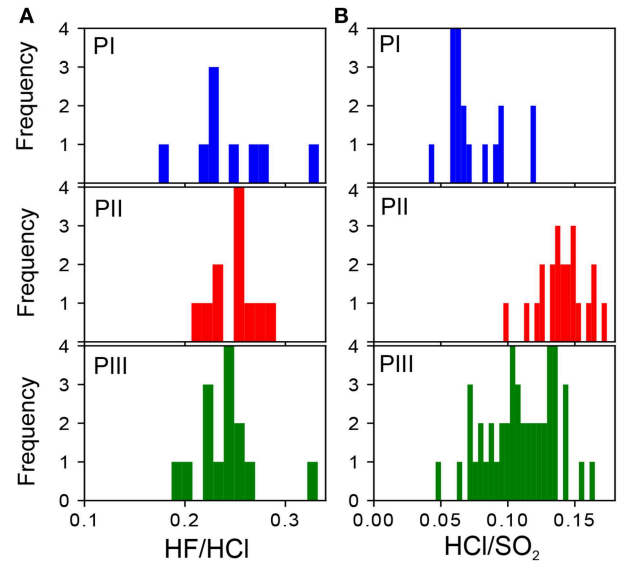

FIGURE 3 | Histogram of the **(A)** HF/HCl and **(B)** HCl/SO_2 ratios for each periods depicted in **Figure 2**.

TABLE 2 | Statistics of the HCl/SO_2 molecular ratios measured in the Popocatépetl plume over the 4-year record.

HCl/SO_2	Total	Period I Nov.2012–May 2013	Period II Nov.2013–Mar. 2014	Period III Sep. 2014– Dec. 2016
Average	0.11	0.07	0.14	0.11
Max	0.22	0.12	0.17	0.17
Min	0.04	0.04	0.10	0.05
STD	0.03	0.02	0.02	0.03

standard deviations interval are selected for the next iteration and a new trend-line is fitted. Convergence was reached after four iterations. Five outliers were identified, numbered 1–5 in **Figure 4B**, where they clearly coincide (within 1 day) with the main RSAM peaks. Most of them even match with the shifts observed in the RSAM cumulative curve on March 07th, 2013 (J1), March 26th, 2013 (J3), and May 8–9th, 2013 (J5).

These five events are characterized by high HCl/SO_2 ratios (**Figure 4B**), and moderate to high SO_2 fluxes ($\geqslant$3,100 ton/day, **Figure 4A**) compared to the global average over our 4-year record (2,790 ton/day). They occur within 24 h after harmonic and spasmodic tremor crisis and almost continuous explosive activity over several hours (explosions or exhalation trains), which correspond to sporadic dome growth episodes. The extreme high HCl/SO_2 ratio value (0.218 ± 0.004) obtained on August 30th, 2013 coincides with the end of an intense period of seismic and volcanic activity.

During our period II (Nov.2013–Mar.2014), 95% of the HCl/SO_2 ratios are higher than the overall average (0.11), with a mean value of 0.14 (**Table 2**). The variability of the HCl/SO_2 ratio is significant during this period which is characterized by a quiet and rather stable volcanic and seismic activity, with relatively low SO_2 fluxes (mean of 1,990 ton/day). The latter can explain the especially high HCl/SO_2 ratio during this period. During the period III (Sep.2014–Dec.2016) another decreasing trend (slope $= -0.08\%$/day and $R^2 = 0.78$) of the HCl/SO_2 ratio is observed, starting with values very similar to those obtained for the period II (around 0.16), and ending with low values similar to those measured during the period I (around 0.06). This decreasing trend started a few weeks before a renewal of the seismic activity after about a year of very low activity.

4.1.3. SiF_4/SO_2

In our time series, SiF_4/SO_2 was higher than the detection limit for only three eruptive events on March 7th and 26th, 2013 and on March 6th, 2015 (**Figure 2A**-red). The values ranged between $(1.9 \pm 0.5) \times 10^{-3}$ and $(9.9 \pm 0.4) \times 10^{-3}$. SiF_4 was previously measured at Popocatépetl volcano with similar abundances (**Table 3**). It is assumed that SiF_4 is formed in the shallow volcanic system from the reaction: $SiO_2(s) + 4HF(g) \rightarrow SiF_4(g) + 2H_2O$ (1), under low temperature conditions ($\leqslant$600°C), when the exsolved HF reacts with the silicate rocks of the conduit or in the plume by ash-gas interaction during explosions. Though, SiF_4 being seldom measured, the precise context favoring its formation remains to be fully depicted.

Here, we find that every detection of SiF_4 took place while a lava dome obstructed the main crater (based on seismic records, webcams observations of ash venting episodes, CENAPRED reports, and photographs taken during crater overflights). The first SiF_4 event detected (on March 7th, 2013) coincides with an important harmonic and spasmodic tremor episode (**Figures 2**, **4**), associated with a 6 h sustained ash venting episode (exhalation train). It likely corresponds to a sporadic growth phase of the lava dome observed during an overflight on March 4th, 2013, probably initially emplaced around February 10th, 2013 (Gómez-Vazquez et al., 2016). The second SiF_4 event (on March 26th, 2013) coincides with another sustained volcanic activity period (**Figure 2**), with similar characteristics (episode of sustained ash venting and explosive activity) probably reflecting a new growth phase of the above mentioned lava dome. The third SiF_4 event, recorded on March 06th, 2015, also coincides with an important active volcanic phase, punctuated by some episodes of harmonic and spasmodic tremor (the last observed on March 06th, 2015 before the dome destruction) and explosive activity. On March 07th, 2015, a $\geqslant$1h-long explosive crisis (train of explosions), ejected incandescent blocks more than 500 m away from the crater. This phase corresponds to a growth episode of the dome emplaced around February 11th, 2015 (CENAPRED Reports; Gómez-Vazquez et al., 2016) and observed during an overflight on February 27th, 2015 with a diameter of 250 m and at least 40 m in thickness (1.96×10^6 m^3).

4.1.4. HBr/HCl and HBr/SO_2

HBr is too dilute in the plume to be properly detected. We however propose its detection limit as an upper limit for its ratio with HCl and SO_2. For this, a set of 15 spectral windows including the HBr lines R8 to R1 and P1 to P7 of the R and P branches were used in the retrieval strategy, typically consisting

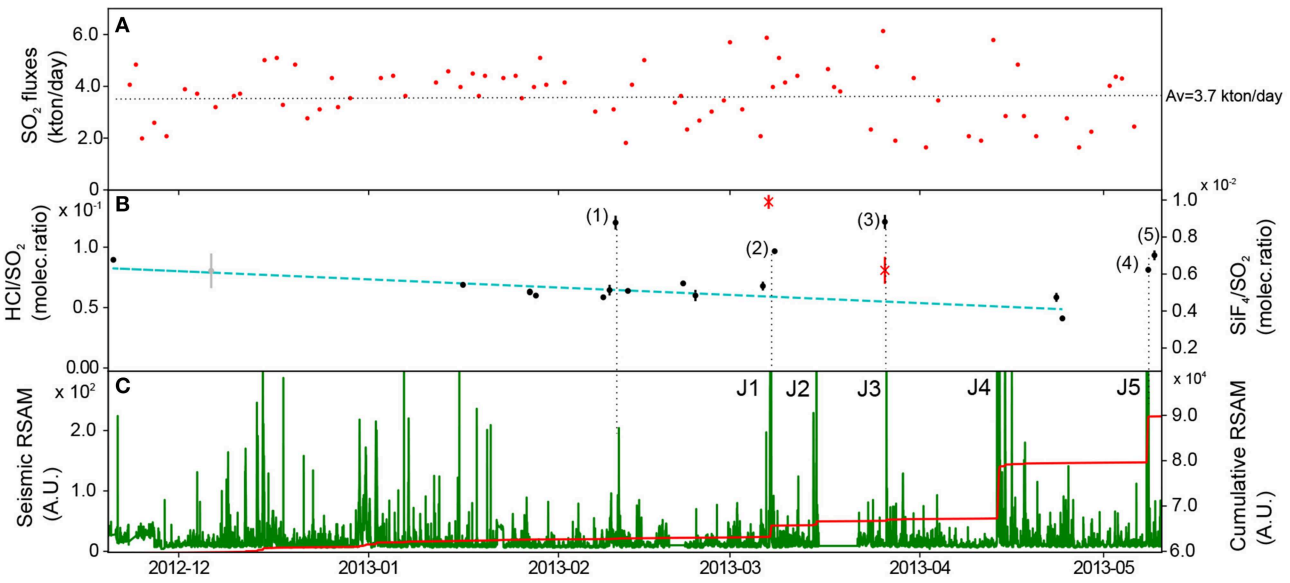

FIGURE 4 | Zoom of the **(A)** SO_2 fluxes, **(B)** HCl/SO_2 (in black and gray), and SiF_4/SO_2 (in red) ratios and **(C)** seismic RSAM time series shown in **Figure 2** from December 2012 to May 2013. In **(B)** the (1–5) points are outliers from the HCl/SO_2 declining trend (cyan) and correspond to ash venting episodes. In **(C)** J1–J5 denote main cumulative RSAM shifts.

in a set of various rather narrow spectral windows (Echle et al., 2000). The error analysis of PROFFIT9.6 includes the estimation of random and systematic errors, and is therefore helpful to estimate the detection limit, either of an individual spectrum or from the analysis of the whole time series. In the high resolution spectra with the highest SO_2 slant columns, we estimated the random error in the HBr retrieval to be about 5.0×10^{14} molec. cm^{-2} and an anomaly can only be detected if the column of a single event exceeds this amount. From this number, the corresponding SO_2 column (4×10^{19} molec. cm^{-2}) and HCl column (4×10^{18} molec. cm^{-2}), we estimated upper limits for the HBr/SO_2 and HBr/HCl ratios, respectively equal to 1.25×10^{-5} and 1.25×10^{-4}.

Assuming a mean Br/Cl ratio of $(2.2 \pm 2.0) \times 10^{-3}$ for arc volcanoes (Gerlach, 2004), we calculated a speculative primitive HBr/SO_2 mean for Popocatépetl from our mean HCl/SO_2 long-term ratio (0.11 ± 0.03). We obtained a HBr/SO_2 range from 1.6×10^{-5} to 5.9×10^{-4} considering the standard deviations. This is surprisingly in the range of the recently reported BrO/SO_2 at Popocatépetl volcano, from 4×10^{-5} to 4×10^{-4} (Fickel and Delgado Granados, 2017), measured at 4 km from the crater using DOAS spectroscopy. Therefore, a significant part of the HBr might have converted into BrO and other bromine species, such as Br_2 (Bani et al., 2009; Gutmann et al., 2018), before our detection.

Such calculations have deeper implications for the halogens degassing at Popocatépetl volcano. Using the maximum of both the theoretical HBr/SO_2 and the measured BrO/SO_2 ratios, we found that if such Br/Cl characterized the Popocatépetl emissions, 68% of HBr would be converted into BrO. This is close to the highest values reported in the literature, for measurements performed at 14 km from the crater of the Ambrym volcano (Bani et al., 2009; Gutmann et al., 2018). This value is abnormally high for measurements at 4 km from the crater (Gutmann et al., 2018), which suggests higher primary Br/Cl and HBr/SO_2 ratios at least for some degassing events at Popocatépetl volcano.

4.2. Variations of the Plume Composition Induced by a Moderate Explosion

Our frequent measurements allow capturing changes in the plume composition preceding and induced by one of the common moderate explosions (mentioned as type 1 in Campion et al., 2018) recorded on March 6th, 2015. **Figures 5A–C**, **6A–C** report the time series of the HF/HCl, HCl/SO_2, and SiF_4/SO_2 ratios and the corresponding correlation plots, which were recalculated point by point from each spectrum. Our measurements started 15 min after the explosion reported by the CENAPRED at 07:30 (local time), and continued up to 6 h afterwards. The explosion was preceded by weak passive degassing and followed by gas puffs (one of the most important occurred at 8:47) punctuating the continuous degassing regime. These degassing regimes were defined in Campion et al. (2018). Using the pictures from the visible camera (taken every minute from the Altzomoni station), the respective arrival times for (i) the first (07:30) explosion plume and (ii) the most important puff (08:47) plume in the instrument optical path are 07:54 (about 10 min after the beginning of the record) and 9:11 (i.e., 24 min travel time for both plumes between emission at the volcano and measurement).

The correlation plots (**Figures 6A–C**) of the different measured gas pairs and the time series of their ratios (**Figures 5A–C**) allow distinguishing different phases during our record. We observe that the pre-explosive and explosive phases (Pa1 and Pa2) are characterized by 10% higher HCl/SO_2

TABLE 3 | Previous measurements of the HCl/SO_2, HF/HCl, SiF_4/SO_2 ratios and SO_2 and HCl fluxes in the Popocatépetl plume.

Date	HCl/SO_2	HF/HCl[a]	$SiF_4/SO_2 \times 10^{-3}$	SO_2 fluxes (ton/day)	HCl fluxes (ton/day)	References
02/19/94	0.14	0.98	–	1,200	100	(Goff et al., 1998, 2001)—alkaline traps
05/04/94	0.21	0.80	–	900	110	(Goff et al., 1998, 2001)—alkaline traps, (Delgado-Granados et al., 2001; Roberge et al., 2009)
07/02/94	0.13	1.37	–	3,100	220	(Goff et al., 1998, 2001)—alkaline traps
11/05/94	0.12	0.64	–	1,260	90	(Goff et al., 1998, 2001)—alkaline traps
12/21/94	0.14	0.18	–	–	–	(Goff et al., 1998, 2001)—alkaline traps
12/21/94 – 06/30/95	–	–	–	3,470	–	(Delgado-Granados et al., 2001)—COSPEC
12/24/94	0.18	0.58	–	3,960	400	(Goff et al., 1998, 2001)—alkaline traps
03/05/96[b]	0.16	0.018	–	–	–	(Goff et al., 1998, 2001)—alkaline traps
03/07/96	0.37	0.18	–	12,900	2,700	(Goff et al., 1998, 2001)—alkaline traps
Average 96	0.17	0.29	–	–	–	(Goff et al., 1998, 2001)—alkaline traps
03/25/96 – 12/29/96	–	–	–	11,000	–	(Delgado-Granados et al., 2001)— COSPEC
02/21/97	–	–	1.0	–	–	(Goff et al., 1998, 2001; Love et al., 1998)—FTIR
02/23/97	0.19	0.73	1.7	–	–	(Goff et al., 1998, 2001; Love et al., 1998)—FTIR
02/24/97	–	–	2.4	2,000	260	(Goff et al., 1998, 2001; Love et al., 1998)—FTIR
02/26/97	–	–	1.0	60,000	7,800	(Goff et al., 1998, 2001; Love et al., 1998)—FTIR
02/27/97	0.23	0.27	–	13,000	1,700	(Goff et al., 1998, 2001)—FTIR
01/17/97 – 05/15/97	–	–	–	12,930	–	(Delgado-Granados et al., 2001)—COSPEC
02/12/98	0.32	0.34	–	1,030	190	(Goff et al., 1998, 2001)—FTIR
02/13/98	0.28	0.32	–	2,710	430	(Goff et al., 1998, 2001)—FTIR
12/01/07	0.05 ± 0.001	0.08 ± 0.01	–	–	–	(Stremme et al., 2011), (Erupt. event)
12/01/07	–	0.04 ± 0.02	–	–	–	(Stremme et al., 2011), (Erupt. event)
12/01/07	–	0.16 ± 0.01	–	–	–	(Stremme et al., 2011), (Erupt. event)
11/17/08	0.15 ± 0.002	0.24 ± 0.01	0.39 ± 0.02–2.56 ± 0.30	–	–	(Stremme et al., 2011, 2012) (Passive degassing)
05/12	0.10	–	–	–	–	Stremme (unpublished data)
01-06/15	–	–	0.1-1.2	–	–	(Taquet et al., 2017)
2012-2016	0.11 ± 0.03	0.24 ± 0.03	1.9 ± 0.5–9.9 ± 0.4	2,790	–	This work
2012-2013(P1)	0.07 ± 0.02	0.24 ± 0.04	6.2 ± 0.7–9.9 ± 0.4	3,680	150	This work (Active period with extrusive activity)
2013-2014(P2)	0.14 ± 0.02	0.25 ± 0.02	–	1,990	160	This work (Quiet episode)
2014-2016(P3)	0.11 ± 0.02	0.24 ± 0.03	1.9 ± 0.5	2,702	167	This work (Active period with renewal of extrusive activity)

[a] *Between 1994 and 1998 HF/HCl is estimated from SO_2/HCl and SO_2/HF ratios.*
[b] *Renewal of extrusive activity (first lava dome observed in March 1996).*

ratios [**Figures 5A**, **6A**, slope (a) $= 0.121 \pm 0.002$, $R^2 = 0.997$] than those of the post explosive phases (Pa3 and Pa4) [slope (b) $= 0.110 \pm 0.001$, $R^2 = 0.997$], which suggests that the post explosive plume is richer in SO_2. HF/HCl variation rates (slope) are similar during Pa1, Pa2, and Pa4 (**Figure 6B**). The post explosive phase (Pa3) is distinguished from the others by much higher SiF_4/SO_2 ratios and variation rates [slope (f) $= 0.022 \pm 0.005$, $R^2 = 0.94$, **Figures 6C**, **5C**] than those of the other phases [slope (e) $= 0.0006 \pm 0.0006$, $R^2 = 0.46$] and comparatively 50% lower HF columns for equivalent HCl columns. The SiF_4/HF ratio is indirectly calculated from the previously reported ratios. The correlation plot of the SiF_4/HCl vs. HF/HCl ratios and the SiF_4/HF time series are reported in **Figures 6D**, **5D**, respectively. A good correlation [trend (f), $R^2 = 0.94$] is found between these ratios, defining a variation rate (slope) of -0.24 ± 0.02, in agreement with the molar balance of the reaction (1) (see section 4.1.3), indicating that the fluorine species are conserved. This result suggests that over the complete record no appreciable quantities of other F-species (e.g., CaF_2, $CaSiF_6$, NaF; Delmelle et al., 2018) than HF and SiF_4 are implied in the fluorine transformation.

5. DISCUSSION

5.1. Insights Into the Origin of the Moderate Explosions at Popocatépetl Volcano

The triggering mechanisms of one of the most common type of explosions at Popocatépetl are explored here, using our daily HCl/SO_2, SiF_4/SO_2, HF/HCl, and SiF_4/HF time series. These

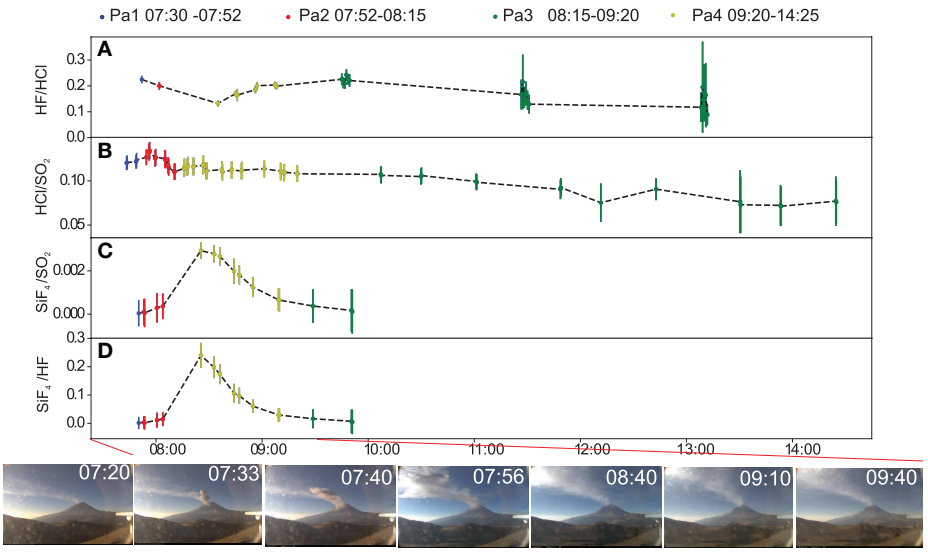

FIGURE 5 | Time series of **(A)** HF/HCl, **(B)** HCl/SO_2, and **(C)** SiF_4/SO_2 ratios acquired on March 6th, 2015 at Popocatépetl volcano. The time axis corresponds to the measurement time, where the plume of the 07:30 a.m. explosion was measured at 07:54. The different colors correspond to the different periods mentioned in the text, Pa1 (07:30–07:52) in blue, Pa2 (07:52–08:15) in red, Pa3 (08:15–09:20) in yellow, and Pa4 (09:20–14:25) in green. **(D)** SiF_4/HF time series calculated from the previously mentioned ratios for the different periods.

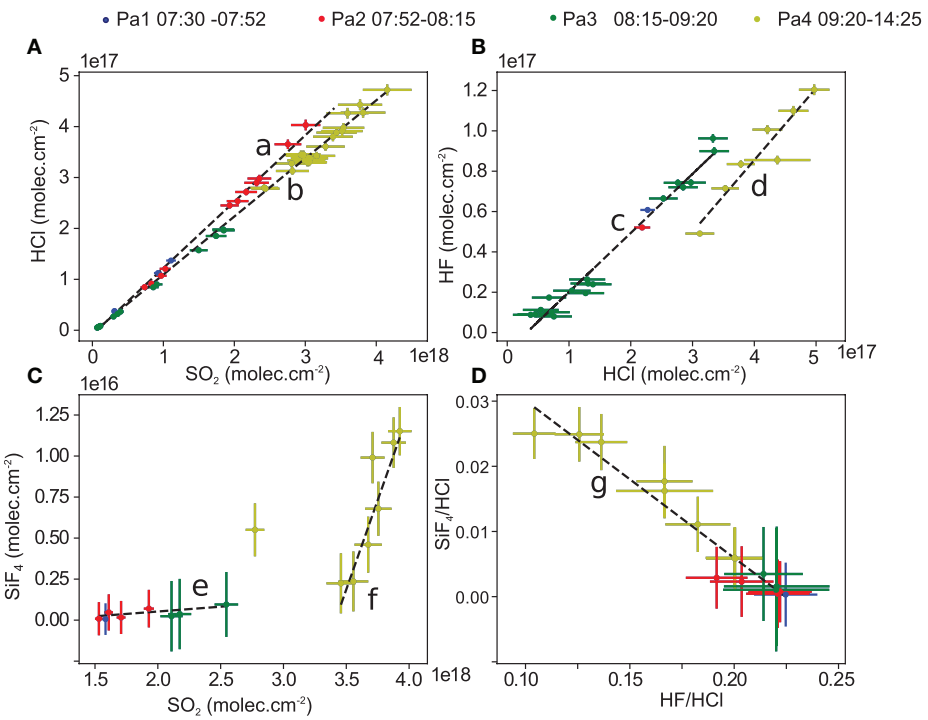

FIGURE 6 | Correlation plots of **(A)** HCl vs. SO_2, **(B)** HF vs. HCl, **(C)** SiF_4 vs. SO_2, and **(D)** SiF_4/HCl vs. HF/HCl several minutes preceding, during and several hours after the detection of an explosion occurring on March 6th, 2015 at 07:30 a.m. The different colors correspond to the periods mentioned in **Figure 5**.

events generally mark important breakdowns in the lava domes growth, causing their partial or total destruction. Some recent geochemical studies have used the SiF_4/HF ratios as a proxy to detect changes in the gas temperature beneath lava domes (Love et al., 1998; Stremme et al., 2012). A common hypothesis is that the dome cooling and an overpressure beneath the dome should drive the vulcanian explosions at the Popocatépetl volcano (Love et al., 1998; Stremme et al., 2012). Such hypothesis has recently

been challenged by high temporal resolution measurements of proxies to the permeability of Popocatépetl domes (Taquet et al., 2017; Campion et al., 2018), showing that the SO_2 fluxes only decreased minutes before explosions, a time frame incompatible with the cooling and solidifying of lava domes. High temporal resolution measurements such as those presented here during March 6th, 2015 provide valuable information on the variability of the HF/HCl, SO_2/HCl, SiF_4/SO_2, and SiF_4/HF ratios several minutes before and up to several hours after typical explosive events. The four correlation plots (**Figure 6**) and the time series (**Figure 5**) presented suggest the existence of various regimes during the same episode, in which different physical and chemical processes predominate:

(i) The first two phases (Pa1 and Pa2) have higher HCl/SO_2 ratios (**Figures 5**, **6**) than the later phases (Pa3 and Pa4). Therefore, the halogen species, which predominate in the volcanic plume at the beginning of the explosion, reveal a momentaneously higher contribution of the shallow degassing.

(ii) The lower HCl/SO_2 ratios observed during the last two phases (Pa3 and Pa4), following the trend (b) in **Figure 6A**, reflect a higher contribution of the deeper exsolved SO_2-rich gas. This explosive phase releases more ash and a large quantity of condensed gases, visible in the fourth photograph in **Figure 5**.

(iii) The measurements performed in the concentrated plume (Pa3) display a specific trend in the HF/HCl (d) and SiF_4/SO_2 (f) correlation plots, which we explain by the formation of SiF_4 from HF.

(iv) The SiF_4/HCl and HF/HCl correlation observed in **Figure 6D** reflects the conservation of fluorine during the whole record.

The presence of SiF_4 in the Popocatépetl's explosion plumes was mainly explained by the release of SiF_4-enriched gas pockets produced by the HF percolation through the lava dome obstructing the crater (Love et al., 1998; Stremme et al., 2011; Taquet et al., 2017). Taquet et al. (2017) observed both prolonged periods (several hours) with a higher base level of SiF_4/SO_2 ratios (likely supporting such a primary production), occasionally preceding the explosions, and sharp SiF_4/SO_2 spikes within periods of high conduit permeability (which rather support the gas-ash interactions). The detection of the primary SiF_4 production (HF percolation through the conduit vs. secondary ash-gas interaction) with our measurements configuration would require the combination of various factors such as an initial strong HF degassing, a little permeable lava dome to improve the HF-silicate interaction (Taquet et al., 2017) and an efficient transport toward the measurement locus. In the case of March 06th measurements, the delay (more than 20 minutes) between the detection of the explosive plume and our significant detection of SiF_4 would imply a special wind scenario (gradient with altitude generating the late arrival of the early emitted SiF_4-rich gas) and low gas mixing to consider SiF_4 as resulting from a primary production. However the delay is more likely explained by the in-plume SiF_4 production from ash.

5.2. Long-Term Evolution of the Popocatépetl Plume Composition

The 4-year time series of HCl/SO_2, HF/HCl, and SiF_4/SO_2 ratios of the Popocatépetl's plume presented here give an overview of its long-term variability during both eruptive and quiescent episodes. **Table 3** summarizes the results from this work together with previous studies using direct sampling, alkaline traps and FTIR techniques. The fairly constant HF/HCl ratio over our record, averaging 0.24 ± 0.03 (min = 0.17; max = 0.33) complies with the HF/HCl average reported by Goff et al. (1998) in 1996 using alkaline traps, and FTIR measurements performed between 1997 and 2008 (average = 0.24; min = 0.02; max = 0.73). These ratios belong to the range defined by Aiuppa et al. (2009) for volatile-rich arc volcanism. The HCl/SO_2 ratios, averaging 0.11 ± 0.03 (min = 0.04; max = 0.22) are also very close to the vast majority of the previous measurements since 1994 (average = 0.17; min = 0.05; max = 0.37; **Table 3**). The SiF_4/SO_2 ratios found for this study (from $(1.9 \pm 0.5) \times 10^{-3}$ to $(9.9 \pm 0.4) \times 10^{-3}$) are in the same order of magnitude as the previously reported values (**Table 3**). The small number of SiF_4 detections during our 4-years time series, compared to that reported in a previous study (Taquet et al., 2017), is probably due to the SiF_4 dilution downwind. The atmospheric chemistry, as well as gas-ash-aerosols interactions, have been proposed to alter the magmatic composition of volcanic plumes (Notsu and Mori, 2010; Martin et al., 2012; Maters et al., 2016). Each individual gas ratio of our dataset corresponds to the slope of well linearly correlated ($R \geqslant 0.8$) gas columns pairs of specific degassing events, thus gas plumes with highly inhomogeneous composition would be filtered out.

The high HCl/SO_2 ratios (averaging 0.14) recorded during the period II, are associated with the lowest SO_2 fluxes and coincide with the unique prolonged low seismic and volcanic activity period of our record (**Figure 2**). The lowest ratios (average $\leqslant 0.1$) observed during the period I and at the end of period III are the lowest since 1994, together with one measurement performed on December 2007 during an eruptive event. The five high HCl/SO_2 ratios, odd to the period I trend, correspond to short extrusive episodes (spasmodic tremor and trains of explosions reported by the CENAPRED, the seismograms are available in http://www.ssn.unam.mx/sismogramas/ppig/). Such events have been characterized by Campion et al. (2018) as strong degassing events with the highest SO_2 fluxes of their survey period. Here, our moderate to high OMI-derived fluxes do not necessarily capture the high SO_2 fluxes of the extrusion phases (generally a few hours long). In any case, the anomalously high HCl/SO_2 ratios (for high to moderate SO_2 fluxes) reflect the shallow exsolution of the halogens during the magma ascent. This observation is in agreement with previous observations for other volcanoes during dome growth episodes (Edmonds et al., 2001).

The HCl/SO_2 decreasing trend observed during the period I (**Figure 2B**) reaches the lowest ratios of the whole time series in April 2013, and coincides with important SO_2 fluxes (average of 3,680 ton/day, **Figure 2C**) compared to those of the period II (average of 1,990 ton/day). This period of higher SO_2 fluxes is part of a more global progressive increase, initiated mid 2011, representing the most important long-term SO_2 flux

variation since 2005 (Carn et al., 2017). The SO_2 fluxes reached and maintained a maximum of around 4,750 ton/day between December 2012 and March 2013, declining to a base-level on September 2013, which is at least twice that of 2006. The injection and mixing of a mafic gas-rich magma in the deep system, eventually assisted by basement assimilation (Goff et al., 1998), is a plausible hypothesis to explain such a global increase of the SO_2 fluxes after 2011, associated with the above-described low HCl/SO_2 ratios (period I). This hypothesis is supported in Espinasa Pereña (2012), describing the main activity steps at Popocatépetl volcano since 1994. The declining trend of the ratio from November 2012 to April 2013 likely reflects a progressive HCl depletion of the gas plume post-2011 magma melange.

From the SO_2 fluxes and the HCl/SO_2 average ratios, the HCl fluxes are estimated to be around 150 and 160 ton/day for periods I and II, respectively and the increase of the HCl/SO_2 ratio observed between the period I and II is due to the reduction of the SO_2 fluxes. The SO_2 fluxes began to decline after an important prolonged peak (E1) between March 7th and 16th, 2013. The E1 peak coincides with a period of intense vulcanian explosions and sometimes trains of explosions, probably reflecting the ultimate extrusive phase of a lava dome growth initiated in February 2013, and which was destroyed several days after (Gómez-Vazquez et al., 2016). We interpret the sharp decline in SO_2 fluxes after E1 as the result of the self-compaction of the plug and/or collapse of parts of the shallow conduit after its strong degassing. The overall declining trend of SO_2 fluxes is finalized by an important prolonged peak (E2), observed between July 3th and August 11th, 2013. This period initiates with the strongest seismic crisis and shift of cumulative RSAM (J5) of our record (between July 3rd and 17th, 2013) and coincides with the destructive phase of a lava dome observed for the last time on July 7th, 2013, followed by the formation of a new crater 200 m wide and 30 m deep observed on July 15th, 2013. The new inner crater remained similar until October 2014 (CENAPRED reports).

The integration of the E2 degassing peak roughly represents 70% of the "missing" SO_2 flux during the progressive obstruction of the conduit between mid-March and June 30th 2013 (difference between the measured SO_2 fluxes and a hypothetical degassing scenario, assuming a constant amount of emissions, based on the fluxes measured between December 2012 and March 2013). Considering the uncertainties on both the OMI-derived SO_2 fluxes and the duration of the periods taken into account for this calculation, the SO_2 peak release (E2) is of the same order of magnitude as the estimated missing SO_2 flux. The E2 SO_2 peak corresponds to the sudden release of the gas accumulated beneath the less permeable plug during the conduit obstruction. The formation of the deep crater after the strong SO_2 discharge (peak E2) probably reflects the main phase of the plug subsidence and the conduit collapse. We speculate that the conduit edges were previously progressively weakened by alternating gas compression and decompression cycles, generating stress and rock alteration during the sustained degassing period.

The sudden decrease of pressure after the main release of accumulated gases (E2) between mid-March and June 30th of 2013 likely provoked the conduit to collapse, and momentarily diminished the shallow system permeability and the SO_2 fluxes between July 17th and August 11th, 2013. We expect that the long-term low SO_2 base-level, combined with high HCl/SO_2 observed during the period II, and coinciding with the low seismic and volcanic activity would rather reflect a late stage degassing of the post-2011 melange. The magma degassing at shallow depth (a shallow reservoir was estimated at a depth of 6 km by Roberge et al., 2009) progressively increases its viscosity and density, damping the magmatic ascension and extrusive activity. The volcanic activity indeed remained at very low levels until the end of 2014, with the extrusion of only a few domes of small volumes (CENAPRED reports; Gómez-Vazquez et al., 2016). The renewal of degassing on October 20th, 2014 is coeval with a short exhalation train and tremor ($\leqslant$4 h long), associated with the growth phase of a new lava dome, the largest of 2014 (Gómez-Vazquez et al., 2016), observed on November 6th during an overflight. The internal pressure of the magmatic system has apparently increased sufficiently to open a new pathway toward the surface. This is highlighted by a renewed degassing consisting in moderate SO_2 fluxes and high HCl/SO_2 ratios similar to those observed during the period II.

The very high HCl/SO_2 ratios exhibited at the beginning of this degassing event, in spite of moderate SO_2 fluxes, indicate that (1) the degassing takes place at a rather shallow level in the magmatic system, and/or (2) the magma is depleted in SO_2 with respect to the period I. In our opinion, this is consistent with the very low seismic activity over the preceding year and indicates that the emitted gases proceed from the 2013 stalling magma batch. The uppermost part of the magma column is the most readily cooled down and prone to crystallization. We speculate that the lesser activity over the year 2014 and the stalling of the magma column enhanced crystallization, which might have resulted in a second boiling episode (Blake, 1984). The latter would have considerably modified the physical properties of the magma (temperature, density, viscosity, vesicularity) and allowed the renewal of degassing. The highest HCl/SO_2 ratios were maintained until the actual resumption of the extrusive activity, dragging the whole magma column toward the surface, and thus progressively implying deeper magmas in the degassing, resulting in the observed declining trend in the HCl/SO_2 time series and the moderate SO_2 fluxes over the years 2015–2016. The exceptionally high SO_2 peak fluxes observed in January 2016 coincide with some of the most violent ash venting episodes of the survey period.

6. CONCLUDING REMARKS

In this work we present a 4-year study on the chemical composition of a volcanic plume with high frequency measurements. The variability of the HCl/SO_2, HF/HCl and SiF_4/SO_2 molecular ratios of the Popocatépetl volcano was determined from solar absorption infrared spectra recorded from a fixed site. The results are in good agreement with measurements reported previously since 1996. However, our long-term time series combined with seismic data and SO_2 fluxes records allowed us deciphering the symptoms of variations in the volcanic activity. While the HF/HCl ratio does not significantly vary for our dataset, the long-term variability of the HCl/SO_2 ratio highly depends on the volcanic (and seismic) activity.

Combining these results with satellite SO_2 fluxes, seismic RSAM and visual observations we suggest that the long-term variability of the HCl/SO_2 ratios results from changes in the shallow plumbing system following the inferred 2011 mafic magma injection. Our study started at the end of 2012, during the late degassing of the post-2011 melange, characterized by a decreasing HCl/SO_2 ratio and strong SO_2 fluxes over several months. Following this period, both the SO_2 fluxes and the volcanic activity drastically decreased for more than a year, reflecting, in our opinion, the progressive densification and crystallization of the melange, damping the extrusive activity. The activity resumes at the end of 2014 with moderate SO_2 fluxes and high HCl/SO_2, progressively decreasing over 2015–2016.

The high temporal resolution of these measurements also captures the plume composition changes preceding and induced by an explosive event at Popocatépetl volcano. Two phases were distinguished, for which different HCl/SO_2 slopes were measured. We propose that the first phase of the explosion implied a higher contribution of the shallow plug degassing while the second phase released an increased contribution of the deeper system. Lava dome-HF or ash-HF interactions within the volcanic plume after the explosion may explain the measured SiF_4/SO_2 and HCl/HF ratios during and after the event. The anti-correlation between SiF_4/HCl and HF/HCl and their slope of $-\frac{1}{4}$ proves the conservation of the fluorine species ($SiF_4 + HF$). This expected result ($0 = -0.25 \times 4 + 1$) confirms the high quality of the individual solar absorption measurements providing a valid basis for further volcanological interpretations. Future work will aim to validate all these observations using complementary techniques, such as a UV-camera to monitor the SO_2 flux more precisely and with higher temporal resolution and more detailed seismic analysis (Salerno et al., 2018). Moreover, attempts to retrieve the emitted CO_2 using solar absorption measurements (Butz et al., 2017) could help to decipher the deeper origin of the variability in the gas composition data measured in the volcanic plume.

AUTHOR CONTRIBUTIONS

NT and WS: gas measurements, gas retrievals, solar absorption spectroscopy, and manuscript writing. JB, AB, BS, CR, and MG: gas retrieval and gas absorption spectroscopy. RC: SO_2 fluxes and discussion. TBo: discussion and contribution to the manuscript writing. AN-T and RE-P: seismic data process. TBl and FH: gas retrieval and gas absorption spectroscopy.

ACKNOWLEDGMENTS

We acknowledge the reviewers G. Tamburello and M. Caroll, the editor N. Bobrowski, and the Chief editor V. Acocella for their thorough review which contributed to significantly improve the quality of the manuscript. We acknowledge the technical personnel of the Centro de Ciencias de la Atmósfera (CCA-UNAM) for maintaining the instruments, in particular H. Sotto, D. Flores, O. López, A. Rodriguez, W. Gutiérrez López, L.M. García y Espinosa de los Reyes. We wish to thank D. Legrand from the Institute of Geophysics (UNAM, Mexico) for fruitful discussions and CENAPRED for providing the seismic data. The financial support through UNAM-DGAPA IN107417 & IN112216 and CONACYT 275239 & 290589 grants is acknowledged. NT and TBo also thank the stipend given by the Mexican Foreign Affairs Department (Secretaría de Relaciones Exteriores) and its AMEXCID program.

REFERENCES

Aiuppa, A., Baker, D., and Webster, J. (2009). Halogens in volcanic systems. *Chem. Geol.* 263, 1–18. doi: 10.1016/j.chemgeo.2008.10.005

Arambula, R., Valdes-Gonzalez, C., Varley, N., Reyes-Pimentel, T. A., and Juarez-Garcia, B. (2016). Tremor and its duration-amplitude distribution at Popocatépetl volcano, Mexico. *Geophys. Res. Lett.* 43, 8994–9001. doi: 10.1002/2016GL070227

Bagnato, E., Aiuppa, A., Bertagnini, A., Bonadonna, C., Cioni, R., Pistolesi, M., et al. (2013). Scavenging of sulphur, halogens and trace metals by volcanic ash: the 2010 Eyjafjallajökull eruption. *Geoch. Cosmochim. Acta* 103, 138–160. doi: 10.1016/j.gca.2012.10.048

Bani, P., Oppenheimer, C., Tsanev, V., Carn, S., Cronin, S., Crimp, R., et al. (2009). Surge in sulphur and halogen degassing from ambrym volcano, Vanuatu. *Bull. Volcanol.* 71, 1159–1168. doi: 10.1007/s00445-009-0293-7

Battaglia, A., de Moor, J. M., Aiuppa, A., Avard, G., Bakkar, H., Bitetto, M., et al. (2019). Insights into the mechanisms of phreatic eruptions from continuous high frequency volcanic gas monitoring: Rincón de la Vieja volcano, Costa Rica. *Front. Earth Sci.* 6:247. doi: 10.3389/feart.2018.00247

Baylon, J. L., Stremme, W., Grutter, M., Hase, F., and Blumenstock, T. (2017). Background CO_2 levels and error analysis from ground-based solar absorption IR measurements in Central Mexico. *Atmos. Measure. Tech.* 10, 2425–2434. doi: 10.5194/amt-10-2425-2017

Blake, S. (1984). Volatile oversaturation during the evolution of silicic magma chambers as an eruption trigger. *J. Geophys. Res.* 89, 8237–8244. doi: 10.1029/JB089iB10p08237

Bluth, G., Casadevall, T., Schnetzler, C., Doiron, S., Walter, L., Krueger, A., et al. (1994). Evaluation of sulfur dioxide emissions from explosive volcanism: the 1982-1983 eruptions of Galunggung, Java, Indonesia. *J. Volcanol. Geother. Res.* 63, 243–256. doi: 10.1016/0377-0273(94)90077-9

Boudon, G., Balcone-Boissard, H., Villemant, B., and Morgan, D. J. (2015). What factors control superficial lava dome explosivity? *Sci. Rep.* 5:14551. doi: 10.1038/srep14551

Butz, A., Dinger, A. S., Bobrowski, N., Kostinek, J., Fieber, L., Fischerkeller, C., et al. (2017). Remote sensing of volcanic CO_2, HF, HCl, SO_2, and BrO in the downwind plume of Mt. Etna. *Atmos. Measure. Tech.* 10, 1–14. doi: 10.5194/amt-10-1-2017

Campion, R. (2014). New lava lake at Nyamuragira volcano revealed by combined ASTER and OMI SO_2 measurements. *Geophys. Res. Lett.* 41, 7485–7492. doi: 10.1002/2014GL061808

Campion, R., Delgado-Granados, H., Legrand, D., Taquet, N., Boulesteix, T., Pedraza-Espitía, S., et al. (2018). Breathing and coughing: the extraordinarily high degassing of Popocatépetl volcano investigated with an SO_2 camera. *Front. Earth Sci.* 6:163. doi: 10.3389/feart.2018.00163

Carn, S., Fioletov, V., McLinden, C., Li, C., and Krotkov, N. (2017). A decade of global volcanic SO_2 emissions measured from space. *Sci. Rep.* 7:44095. doi: 10.1038/srep44095

Delgado-Granados, H., Cardenas Gonzalez, L., and Piedad Sanchez, N. (2001). Sulfur dioxide emissions from Popocatépetl volcano (Mexico): case study of a high-emission rate, passively degassing erupting volcano. *J. Volcanol. Geotherm. Res.* 108, 107–120. doi: 10.1016/S0377-0273(00)00280-8

Delmelle, P., Wadsworth, F. B., Maters, E. C., and Ayris, P. M. (2018). High temperature reactions between gases and ash particles in volcanic eruption plumes. *Rev. Mineral. Geochem.* 84, 285–308. doi: 10.2138/rmg.2018.84.8

Echle, G., von Clarmann, T., Dudhia, A., Flaud, J.-M., Funke, B., Glatthor, N., et al. (2000). Optimized spectral microwindows for data analysis of the michelson

interferometer for passive atmospheric sounding on the environmental satellite. *Appl. Opt.* 39, 5531–5540. doi: 10.1364/AO.39.005531

Edmonds, M., Pyle, D., and Oppenheimer, C. (2001). A model for degassing at the Soufrière Hills volcano, Montserrat, West Indies, based on geochemical data. *Earth Planet. Sci. Lett.* 186, 159–173. doi: 10.1016/S0012-821X(01)00242-4

Endo, E. T., and Murray, T. (1991). Real-time seismic amplitude measurement (RSAM): a volcano monitoring and prediction tool. *Bull. Volcanol.* 53, 533–545. doi: 10.1007/BF00298154

Espinasa Pereña, R. (2012). *Historia de la Actividad del Volcán Popocatépetl 17 Años de Erupciones.* Mexico: CENAPRED.

Fickel, M., and Delgado Granados, H. (2017). On the use of different spectral windows in DOAS evaluations: effects on the estimation of SO_2 emission rate and mixing ratios during strong emission of Popocatépetl volcano. *Chem. Geol.* 462, 67–73. doi: 10.1016/j.chemgeo.2017.05.001

Francis, P., Chaffin, C., Maciejewski, A., and Oppenheimer, C. (1996). Remote determination of SiF_4 in volcanic plumes: a new tool for volcano monitoring. *Geophys. Res. Lett.* 23, 249–252. doi: 10.1029/96GL00022

Gerlach, T. M. (2004). Volcanic sources of tropospheric ozone-depleting trace gases. *Geochem. Geophys. Geosyst.* 5:Q09007. doi: 10.1029/2004GC000747

Gisi, M., Hase, F., Dohe, S., Blumenstock, T., Simon, A., and Keens, A. (2012). XCO_2-measurements with a tabletop FTS using solar absorption spectroscopy. *Atmos. Measure. Tech.* 5, 2969–2980. doi: 10.5194/amt-5-2969-2012

Goff, F., Janik, C. J., Delgado, H., Werner, C., Counce, D., Stimac, J. A., et al. (1998). Geochemical surveillance of magmatic volatiles at Popocatépetl volcano, Mexico. *Geol. Soc. Am. Bull.* 110, 695–710. doi: 10.1130/0016-7606(1998)110<0695:GSOMVA>;2.3.CO;2

Goff, F., Love, S. P., Warren, R., Counce, D., Obenholzner, J., Siebe, C., et al. (2001). Passive infrared remote sensing evidence for large, intermittent CO_2 emissions at Popocatépetl volcano, Mexico. *Chem. Geol.* 177, 133–156. doi: 10.1016/S0009-2541(00)00387-9

Gómez-Vazquez, A., De la Cruz-Reyna, S., and Mendoza-Rosas, A. T. (2016). The ongoing dome emplacement and destruction cyclic process at Popocatépetl volcano, central mexico. *Bull. Volcanol.* 78:58. doi: 10.1007/s00445-016-1054-z

Grutter, M., Basaldud, R., Rivera, C., Harig, R., Junkerman, W., Caetano, E., et al. (2008). SO_2 emissions from Popocatépetl volcano: emission rates and plume imaging using optical remote sensing techniques. *Atmos. Chem. Phys.* 8, 6655–6663. doi: 10.5194/acp-8-6655-2008

Gutmann, A., Bobrowski, N., Roberts, T., Rüdiger, J., and Hoffmann, T. (2018). Advances in bromine speciation in volcanic plumes. *Front. Earth Sci.* 6:24. doi: 10.3389/feart.2018.00213

Hase, F., Hannigan, J., Coffey, M., Goldman, A., Hopfner, M., Jones, N., et al. (2004). Intercomparison of retrieval codes used for the analysis of high-resolution, ground-based FTIR measurements. *J. Quant. Spectrosc. Radiat. Transfer* 87, 25–52. doi: 10.1016/j.jqsrt.2003.12.008

Hirabayashi, J., Ossaka, J., and Ozawa, T. (1982). Relationship between volcanic activity and chemical composition of volcanic gases; a case study on the Sakurajima Volcano. *Geochem. J.* 16, 11–21. doi: 10.2343/geochemj.16.11

Lee, S., Kang, N., Park, M., Hwang, J. Y., Yun, S. H., and Jeong, H. Y. (2018). A review on volcanic gas compositions related to volcanic activities and non-volcanological effects. *Geosci. J.* 22, 183–197. doi: 10.1007/s12303-017-0056-y

Love, S. P., Goff, F., Counce, D., Siebe, C., and Delgado, H. (1998). Passive infrared spectroscopy of the eruption plume at Popocatépetl volcano, Mexico. *Nature* 396, 563–567. doi: 10.1038/25109

Manga, M., Mitchell, S. J., Degruyter, W., and Carey, R. J. (2018). Transition of eruptive style: pumice raft to dome-forming eruption at the havre submarine volcano, Southwest Pacific Ocean. *Geology* 46, 1075–1078. doi: 10.1130/G45436.1

Martel, C., and Schmidt, B. C. (2003). Decompression experiments as an insight into ascent rates of silicic magmas. *Contrib. Mineral. Petrol.* 144, 397–415. doi: 10.1007/s00410-002-0404-3

Martin, R., Wheeler, J., Ilyinskaya, E., Braban, C., and Oppenheimer, C. (2012). The uptake of halogen (HF, HCl, HBr and HI) and nitric (HNO_3) acids into acidic sulphate particles in quiescent volcanic plumes. *Chem. Geol.* 296, 19–25. doi: 10.1016/j.chemgeo.2011.12.013

Maters, E. C., Delmelle, P., and Bonneville, S. (2016). Atmospheric processing of volcanic glass: effects on iron solubility and redox speciation. *Environ. Sci. Technol.* 50, 5033–5040. doi: 10.1021/acs.est.5b06281

McCormick, B. T., Herzog, M., Yang, J., Edmonds, M., Mather, T. A., Carn, S. A., et al. (2014). A comparison of satellite-and ground-based measurements of so^2 emissions from tungurahua volcano, ecuador. *J. Geophys. Res.* 119, 4264–4285. doi: 10.1002/2013JD019771

Mori, T., and Notsu, K. (2008). Temporal variation in chemical composition of the volcanic plume from Aso volcano, Japan, measured by remote FT-IR spectroscopy. *Geochem. J.* 42, 133–140. doi: 10.2343/geochemj.42.133

Mori, T., Sato, M., Shimoike, Y., and Notsu, K. (2002). High SiF_4/HF ratio detected in Satsuma-Iwojima volcano's plume by remote FT-IR observation. *Earth Planets Space* 54, 249–256. doi: 10.1186/BF03353024

Notsu, K., and Mori, T. (2010). Chemical monitoring of volcanic gas using remote FT-IR spectroscopy at several active volcanoes in Japan. *Appl. Geochem.* 25, 505–512. doi: 10.1016/j.apgeochem.2010.01.008

Oppenheimer, C., Edmonds, M., Francis, P., and Burton, M. (2002). Variation in HCl/SO_2 gas ratios observed by fourier transform spectroscopy at Soufrière Hills volcano, Montserrat. *Geol. Soc. Lond. Memoirs* 21, 621–639. doi: 10.1144/GSL.MEM.2002.021.01.31

Roberge, J., Delgado-Granados, H., and Wallace, P. J. (2009). Mafic magma recharge supplies high CO_2 and SO_2 gas fluxes from Popocatépetl volcano, Mexico. *Geology* 37:107. doi: 10.1130/G25242A.1

Rothman, L. S., Jacquemart, D., Barbe, A., Benner, D. C., Birk, M., Brown, L., et al. (2005). The HITRAN 2004 molecular spectroscopic database. *J. Quant. Spectrosc. Radiat. Trans.* 96, 139–204. doi: 10.1016/j.jqsrt.2004.10.008

Salerno, G. G., Burton, M., Di Grazia, G., Caltabiano, T., and Oppenheimer, C. (2018). Coupling between magmatic degassing and volcanic tremor in basaltic volcanism. *Front. Earth Sci.* 6:157. doi: 10.3389/feart.2018.00157

Schiavo, B., Stremme, W., Grutter, M., Campion, R., Guarin, C. A., Rivera, C., et al. (2019). Characterization of a UV camera system for So2 measurements from popocatépetl volcano. *J. Volcanol. Geother. Res.* 370, 82–94. doi: 10.1016/j.jvolgeores.2018.09.001

Shinohara, H., Ohminato, T., Takeo, M., Tsuji, H., and Kazahaya, R. (2015). Monitoring of volcanic gas composition at Asama volcano, Japan, during 2004-2014. *J. Volcanol. Geother. Res.* 303, 199–208. doi: 10.1016/j.jvolgeores.2015.07.022

Siebe, C., Abrams, M., Macias, J. L., and Obenholzner, J. (1996). Repeated volcanic disasters in Prehispanic time at Popocatépetl, central Mexico: past key to the future? *Geology* 24:399. doi: 10.1130/0091-7613(1996)024<0399:RVDIPT>2.3.CO;2

Stremme, W., Krueger, A., Harig, R., and Grutter, M. (2012). Volcanic SO_2 and SiF_4 visualization using 2-D thermal emission spectroscopy - Part 1: Slant-columns and their ratios. *Atmos. Measure. Tech.* 5, 275–288. doi: 10.5194/amt-5-275-2012

Stremme, W., Ortega, I., Siebe, C., and Grutter, M. (2011). Gas composition of Popocatépetl Volcano between 2007 and 2008: FTIR spectroscopic measurements of an explosive event and during quiescent degassing. *Earth Planet. Sci. Lett.* 301, 502–510. doi: 10.1016/j.epsl.2010.11.032

Taquet, N., Hernández, I. M., Stremme, W., Bezanilla, A., Grutter, M., Campion, R., et al. (2017). Continuous measurements of SiF_4 and SO_2 by thermal emission spectroscopy: insight from a 6-month survey at the Popocatépetl volcano. *J. Volcanol. Geotherm. Res.* 341, 255–268. doi: 10.1016/j.jvolgeores.2017.05.009

Witter, J. B., Kress, V. C., and Newhall, C. G. (2005). Volcan Popocatépetl, Mexico. Petrology, magma mixing, and immediate sources of volatiles for the 1994 present eruption. *J. Petrol.* 46, 2337–2366. doi: 10.1093/petrology/egi058

Yang, K., Krotkov, N. A., Krueger, A. J., Carn, S. A., Bhartia, P. K., and Levelt, P. F. (2007). Retrieval of large volcanic SO_2 columns from the aura ozone monitoring instrument: comparison and limitations. *J. Geophys. Res. Atmospheres* 112, 24–43. doi: 10.1029/2007JD008825

Conflict of Interest Statement: The authors declare that the research was conducted in the absence of any commercial or financial relationships that could be construed as a potential conflict of interest.

The handling editor declared a past co-authorship with one of the authors FH.